

# Model-independent Reconstruction of UV Luminosity Function and Reionization Epoch

Debabrata Adak,<sup>a,b,c,d</sup> Dhiraj Kumar Hazra,<sup>c,d,e</sup> Sourav Mitra,<sup>f</sup>  
Aditi Krishak<sup>c,g</sup>

<sup>a</sup>Instituto de Astrofísica de Canarias, E-38200 La Laguna, Tenerife, Spain

<sup>b</sup>Departamento de Astrofísica, Universidad de La Laguna, E-38206 La Laguna, Tenerife, Spain

<sup>c</sup>The Institute of Mathematical Sciences, CIT Campus, Chennai 600113, India

<sup>d</sup>Homi Bhabha National Institute, Training School Complex, Anushakti Nagar, Mumbai 400085, India

<sup>e</sup>INAF/OAS Bologna, Osservatorio di Astrofisica e Scienza dello Spazio di Bologna, via Gobetti 101, I-40129 Bologna, Italy

<sup>f</sup>Department of Physics, Surendranath College, 24/2 M. G. Road, Kolkata 700009, India

<sup>g</sup>Department of Physics and Astronomy, University of Southern California, University Park, Los Angeles, CA 90089, USA

E-mail: [adak@iac.es](mailto:adak@iac.es), [dhiraj@imsc.res.in](mailto:dhiraj@imsc.res.in), [hisourav@gmail.com](mailto:hisourav@gmail.com), [krishak@usc.edu](mailto:krishak@usc.edu)

**Abstract.** We conduct a first comprehensive study of the Luminosity Function (LF) using a non-parametric approach. We use Gaussian Process to fit available luminosity data between redshifts  $z \sim 2 - 8$ . Our free-form LF in the non-parametric approach rules out the conventional Schechter function model to describe the abundance-magnitude relation at redshifts  $z = 3$  and 4. Hints of deviation from the Schechter function are also noticed at redshifts 2, 7 and 8 at lower statistical significance. Significant deviation starts for brighter ionizing sources at  $M_{UV} \lesssim -21$ . The UV luminosity density data at different redshifts are then derived by integrating the LFs obtained from both methods with a truncation magnitude of  $-17$ . In our analysis, we also include the first 90 arcmin<sup>2</sup> JWST/NIRCam data at  $z \sim 9 - 12$ . Since at larger magnitudes, we do not find major deviations from the Schechter function, the integrated luminosity density differs marginally between the two methods. Finally, we obtain the history of reionization from a joint analysis of UV luminosity density data along with the ionization fraction data and Planck observation of Cosmic Microwave Background. The history of reionization is not affected by the deviation of LFs from Schechter function at lower magnitudes. We derive reionization optical depth to be  $\tau_{re} = 0.0494_{-0.0006}^{+0.0007}$  and the duration between 10% and 90% completion of ionization process is found to be  $\Delta z \sim 1.627_{-0.071}^{+0.059}$ .

**Keywords:** Galaxy Luminosity function - Gaussian process (GP) - Reionization history

---

## Contents

<b>1</b>	<b>Introduction</b>	<b>1</b>
<b>2</b>	<b>Methodology</b>	<b>2</b>
2.1	Cosmic Reionization	2
2.2	Gaussian Process Regression	4
<b>3</b>	<b>Data sets</b>	<b>4</b>
<b>4</b>	<b>Results</b>	<b>5</b>
4.1	Relation between magnitude and Galaxy UV LF	5
4.2	Evolution of UV Luminosity Density	7
4.3	Constraints on Reionization	10
<b>5</b>	<b>Summary</b>	<b>12</b>
<b>6</b>	<b>Acknowledgement</b>	<b>13</b>

---

## 1 Introduction

The process of cosmic reionization is an outstanding problem in extragalactic astronomy. During the redshifts  $z \sim 6 - 20$  almost all of the hydrogen in the universe became ionized [1–5]. A similar process was followed for helium at a later time and helium reionization was completed at around  $z \sim 2.5 - 3.5$  [6]. For this process, the high-redshift ( $z \gtrsim 6$ ) star-forming galaxies are often considered to be the dominant contributors of ionizing photons since the abundance of quasars dramatically declines at  $z \sim 6$  [7–9]. A variety of theoretical and observational studies have shown that the contribution of Active Galactic Nuclei has a very minimal ( $\lesssim 1\%$ ) contribution to the total ionisation budget at  $z \geq 6$  [10, 11]. Most of the studies suggest that star-forming galaxies inside the low mass halo ( $M_h \lesssim 10^{9.5} M_\odot$ ) are sufficient enough to complete the reionization process [12, 13]. Therefore, their time-dependent abundance, and the redshift evolution of UV luminosity density ( $\rho_{UV}$ ) derived from rest-frame UV luminosity function (LF) of galaxies are of significant interest for understanding reionization history (see, [14]).

Significant advancement has been made in determining the behaviour of LFs at redshifts  $z \sim 4 - 10$  using Hubble Frontier Fields (HFF, [15]) survey data up to magnitude  $\simeq -15$  [16–18]. More recently, the same has been studied in [19, 20] and [21] with galaxy candidates down to magnitude  $\simeq -22$ . However, along with studying the faint end of the UV LF, it is also important to investigate the bright-end shape of LF. While the conventional Schechter function [22] seems to be a good description of the LFs for ionizing candidates at the fainter end of the magnitude, an exponential decline has been reported in their number densities at the bright-end [23]. It is thought to be caused by heating from an active galactic nucleus (AGN, [24]), inefficient cooling of gas inside high-mass dark matter halos at low redshifts [25] etc. Recent works of [26] and [27] found that both double power-law (DPL, [28]) and lensed Schechter function [29] are better fitted to UV luminosity data including brightest galaxy candidates observed in the early data from James Webb Space Telescope (JWST, [30]) and

Great Optically Luminous Dropout Research data of Subaru HSC (GOLDRUSH) (corrected for AGN contribution) respectively. Publications [31] and [32] independently established that LFs are more consistent with DPL at  $z \sim 9 - 10$ . More recent studies in [26, 33] and [34] also reported an excess of number density compared to that described by the Schechter best fit at  $z \sim 4 - 7$ .

In this paper, we address the constraints on reionization history in a two-step process. First, we reconstruct the profile of the LFs using Gaussian process regression (GP), a nonparametric regression method at redshifts  $z \sim 2 - 8$ , and Schechter function model at redshifts  $z \sim 2 - 12$  using the HFF data, early JWST data and HSC data. We compare these model-independent LFs with the conventional Schechter function model of LFs. We derive the UV luminosity densities by integrating LFs, and investigate the redshift evolution of UV luminosity densities derived from both profiles. Finally, we use these luminosity densities to constrain the history of reionization along with jointly fitting two other observational data: the CMB power spectrum data of temperature and polarization anisotropy from Planck observation [4] and neutral hydrogen fraction data from galaxy, quasar and gamma-ray burst observations.

The paper is organised as follows. In section 2 we briefly discuss the reionization process, different functions used and details of Gaussian process regression. In section 3 we describe the ancillary data sets used in this work. In section 4 we present our results for the UV luminosity functions obtained using two different methods, their comparison, derived UV luminosity densities and the corresponding constraints on reionization history. Finally in section 5 we summarise the work.

## 2 Methodology

### 2.1 Cosmic Reionization

The process of reionization of the intergalactic medium (IGM) is a balance between ionization of hydrogen and helium atoms by cosmic photons and recombination of free electrons and protons to form neutral hydrogen and helium. Analytical and numerical modelling of this process traces a long history [13, 35, 36] (see the references therein). The process is studied by the redshift evolution of volume filling factor  $Q_{\text{HII}}$  which is governed by the ionization histories of both hydrogen and helium. The time evolution of  $Q_{\text{HII}}$  is obtained by solving the ordinary differential equation (e.g. [37])

$$\dot{Q}_{\text{HII}} = \frac{\dot{n}_{\text{ion}}}{\langle n_H \rangle} - \frac{Q_{\text{HII}}}{t_{\text{rec}}}, \quad (2.1)$$

where  $\langle n_H \rangle = \frac{X_p \Omega_b \rho_c}{m_H}$  is the mean comoving number density of hydrogen and depends on the primordial mass-fraction of hydrogen  $X_p$ , critical density  $\rho_c$ , baryon density  $\Omega_b$  and  $m_H$  is the mass of atomic hydrogen.  $t_{\text{rec}}$  denotes the average recombination time in the IGM,

$$t_{\text{rec}} = \frac{1}{C_{\text{HII}} \alpha_B(T) \left(1 + \frac{Y_p}{4X_p}\right) \langle n_H \rangle (1+z)^3}, \quad (2.2)$$

where  $\alpha_B(T)$  is the recombination coefficient for hydrogen (we assume the IGM temperature  $T$  to be 20,000 K) and  $Y_p = 1 - X_p$  is the primordial helium abundance. The clumping factor  $C_{\text{HII}}$  accounts for the inhomogeneity of the IGM, and is not very well constrained from

observations. Recent simulations suggest a possible range of  $C_{\text{HII}}$  value from 1 to 6 [38–41]. In this work we use the fixed value of  $C_{\text{HII}} = 3$  [42] for simplicity. The comoving production rate of available ionizing photons in the IGM at some redshift is

$$\begin{aligned}\dot{n}_{\text{ion}} &= \int_{-\infty}^{M_{\text{trunc}}} f_{\text{esc}}(M) \xi_{\text{ion}}(M) \Phi(M) L(M) dM \\ &= \langle f_{\text{esc}} \xi_{\text{ion}} \rangle \rho_{\text{UV}}.\end{aligned}\tag{2.3}$$

This depends on the intrinsic production rate of Lyman continuum (LyC) photons supplied by stellar populations of galaxies, which is parameterized by a numerical factor  $\xi_{\text{ion}}$  to count the ionizing photons per unit UV luminosity, the escape fraction  $f_{\text{esc}}$  and total luminosity density  $\rho_{\text{UV}}$  from star-forming galaxies with a truncation absolute magnitude  $M_{\text{trunc}}$ .  $f_{\text{esc}}$  is a crucial parameter and is not well-constrained from direct observations of LyC photons [43], which is mainly limited to  $z \sim 2 - 4.5$  due to a dramatic increase in the opacity of IGM at high redshifts making direct observation of LyC photons difficult [44]. Moreover, the trend of  $f_{\text{esc}}$  with halo mass is not well understood from theoretical modelling [45–47]. All pre-JWST literatures suggest that a low ionisation efficiency of around  $\log_{10} \xi_{\text{ion}} = 25.2 \text{ Hz erg}^{-1}$  and hence  $f_{\text{esc}}$  of 0.2 [37] that are sufficient to give reionization history consistent with CMB data. However new JWST data suggests a higher  $\xi_{\text{ion}}$  [48] that increases at redshifts higher than  $z \sim 9$  [49, 50]. It is apparent that  $\xi_{\text{ion}}$  and  $f_{\text{esc}}$  are completely degenerate parameters. A recent data-driven model-independent study [51] found that a constant value of  $f_{\text{esc}}$  for  $z \geq 6$  is permitted. Therefore, we take  $f_{\text{esc}}$  as a constant factor and, instead of considering  $\xi_{\text{ion}}$  and  $f_{\text{esc}}$  to be independent parameters, we consider the magnitude-averaged value of  $\langle f_{\text{esc}} \xi_{\text{ion}} \rangle$  as a single parameter in this work.

Luminosity density  $\rho_{\text{UV}}$  is obtained from the luminosity function  $\phi(M_{\text{UV}})$  via integration,

$$\rho_{\text{UV}} = \int_{-\infty}^{M_{\text{trunc}}} \Phi(M) L(M) dM,\tag{2.4}$$

where  $L(M)$  is the luminosity. One can set the truncation magnitude at  $M_{\text{trunc}} = -10$  corresponding to the predicted range of minimum halo-mass that can host star-forming galaxies [52]. However, due to insufficient data at some redshifts at larger magnitudes ( $M_{\text{UV}} > -17$ ), our free-form LFs obtained using GP will be biased to the mean function beyond the range of training data. Therefore, we restrict ourselves to  $M_{\text{trunc}} = -17$ . Accurate estimation of  $\rho_{\text{UV}}$  from UV galaxies requires a careful analysis of the LF profile that can well-describe the number densities of star-forming galaxy samples down to observed limits. The best model of LF in literature is often assumed to be the Schechter function [22],

$$\Phi(M) = 0.4 \ln 10 \phi^* [10^{0.4(M^* - M)}]^{1+\alpha} \exp[-10^{0.4(M^* - M)}]\tag{2.5}$$

parameterized by  $\phi^*$  ( $\text{Mpc}^{-3} \text{mag}^{-1}$ ),  $M^*$  and  $\alpha$ . We find the posterior distributions of Schechter function parameters in redshifts  $z \sim 2 - 12$  using the UV luminosity data sets described in section 3. We also fit same data sets using the non-parametric method discussed in subsection 2.2. We then obtain  $\rho_{\text{UV}}$  corresponding to each of these best-fit LFs using Equation 2.5.

In order to constrain the reionization process, we need to adopt a parametric form [19, 20, 53] or a free-form [54–57] of  $\rho_{\text{UV}}$  evolution to constrain  $\dot{n}_{\text{ion}}$ . The model-independent reconstruction of reionization process in [56] rules out the single power-law [53] form which that is unable to replicate the decline at  $z \sim 8$ . This results in an incorrect value of the

Thomson scattering optical depth. Therefore, in our analysis we use the logarithmic double power law [19, 20] to describe  $\rho_{\text{UV}}$ ,

$$\rho_{\text{UV}} = \frac{2\rho_{\text{UV},z=z_{\text{tilt}}}}{10^{a(z-z_{\text{tilt}})} + 10^{b(z-z_{\text{tilt}})}}, \quad (2.6)$$

where  $\rho_{\text{UV},z=z_{\text{tilt}}}$  is the normalization factor at  $z_{\text{tilt}} \sim 8$ , and  $a$  and  $b$  are the slopes.

Once the evolution of  $Q_{\text{HII}}$  from Eq. 2.1 is determined, we compute the reionization optical depth at redshift  $z$  using

$$\tau_{\text{re}} = \int_0^z \frac{c(1+z')^2}{H(z')} Q_{\text{HII}}(z') \langle n_H \rangle \sigma_T (1 + \eta \frac{Y_p}{4X_p}) dz', \quad (2.7)$$

where  $c$  is the speed of light,  $H(z)$  is the Hubble parameter, and  $\sigma_T$  is the Thomson scattering cross section. Here we assume that helium is singly ionized ( $\eta = 1$ ) at  $z > 4$  and doubly ionized ( $\eta = 2$ ) at  $z \leq 4$  [36].

## 2.2 Gaussian Process Regression

Gaussian process regression is a non-parametric Bayesian regression method. This method has been extensively used in cosmological data analysis [58–60]. A Gaussian process is a collection of random variables such that any finite subset of these random variables has a multivariate Gaussian distribution [61]. A GP is described by its mean and covariance functions, defined as  $\mu(\mathbf{x}) = \mathbb{E}[f(\mathbf{x})]$ , and  $k(\mathbf{x}, \mathbf{x}') = \mathbb{E}[(f(\mathbf{x}) - \mu(\mathbf{x}))(f(\mathbf{x}') - \mu(\mathbf{x}'))]$ , respectively, for a real process  $f(\mathbf{x})$ . In particular, here  $f(\mathbf{x})$  defines the luminosity-magnitude relation guided by data for a given mean function. The covariance function gives the covariance between two random variables and characterizes the covariance matrix having elements  $C_{i,j} = k(x_i, x_j)$ . Given a finite set of training points  $\mathbf{x} = \{x_i\}$ , a function  $f(\mathbf{x})$  evaluated at each  $x_i$  is a Gaussian random variable and the vector  $\mathbf{f} = \{f_i\}$  has a multivariate Gaussian distribution given as  $\mathbf{f} \sim \mathcal{N}(\mu(\mathbf{x}), C(\mathbf{x}, \mathbf{x}))$ . The choice of the covariance functions is important. We choose the Radial Basis Function (RBF) kernel as the covariance function for our analysis, defined as  $k(x_i, x_j) = \sigma_\ell \exp\left(-\frac{(x_i - x_j)^2}{2\ell^2}\right)$ , where  $\sigma_\ell$  and  $\ell$  are the kernel hyperparameters. The  $\sigma_\ell$  is the amplitude parameter that can be thought as an offset that decides the tilt of reconstructed function  $f(\mathbf{x})$  from given mean function and  $\ell$  describes the characteristic length of correlation. Data points act as training points to optimize the hyperparameters and provide posterior prediction along with uncertainty on the predictions for the given test points.

Although GP is a formalism to be used here to study actual trends of data to define the luminosity-magnitude relation, there are practical technicalities regarding the choice of mean function that require special care. In principle, one can choose a zero mean function or any random function to start with. In this study, however, we are particularly interested in checking the validity of the Schechter function to be a correct description of the luminosity-magnitude relation. To test that, we allow the three Schechter function parameters to vary along with the GP hyperparameters,  $\ell$  and  $\sigma_\ell$ . In this way, the hyperparameter posteriors, marginalized over the Schechter function parameters can indicate, in a conservative way, whether the Schechter function is a correct model to address the observational data.

## 3 Data sets

We use rest frame UV luminosity function data for redshifts  $z \sim 2, 3, 4, 5, 6, 7$  derived in [62] using HUDF, HFF, and CANDELS fields and HFF data compiled by [20]. For  $z \sim 4-7$

we add data from Hyper Suprime-Cam (HSC) Subaru Strategic Program (SSP) survey [63]. These data sets are corrected for active galactic nucleus (AGN) contribution and mostly at brighter end of luminosity. For redshifts 8, 9 and 10 we use luminosity function data from [62], [32], [64] and [65]. We also use the data redshift 9 and 12 from JWST [66].

We use neutral hydrogen fraction data to constrain reionization from observations of Ly $\alpha$ -emitting galaxies [46, 67–69], high-redshift quasar spectra [41, 70, 71], gamma ray bursts [72, 73], dark fraction in the spectra of bright quasars [2] and ionized near-zones around high-redshift quasars [74, 75].

From Planck CMB, we use Planck binned `Planck TTTEEE` likelihood with low multipole temperature and polarization likelihoods and the lensing likelihood as discussed in Planck baseline [4].

## 4 Results

### 4.1 Relation between magnitude and Galaxy UV LF

To characterise the galaxy UV LF, we use both Schechter function (Equation 2.5) and GP to fit the luminosity data. We use data for the largest possible range of magnitude,  $-25 < M_{UV} < -14$  wherever available. We use CosmoMc [76] as a generic sampler to explore the parameter space.

For fitting the Schechter function we keep all three parameters  $M^*$ ,  $\phi^*$  and  $\alpha$  free. However, we notice that for  $z > 8$  the data is not able to constrain all the parameters. Therefore, at  $z \geq 9$ , we keep the slope  $\alpha$  fixed at  $-2.35$  following [27] and determine the other two Schechter parameters at  $z \sim 9-12$ . We find the estimated parameters are consistent with previous results of [20, 32, 62]. For  $z \sim 10$  and 12, we fix the prior on  $M_{UV}^*$  as the 68% range obtained in  $z \sim 9$  analysis. In Figure 1 we present posterior distributions of the Schechter function parameters. We fit the free-form of LF using GP with the same data sets keeping GP hyperparameters ( $\ell$  and  $\sigma_\ell$ ) free along with three Schechter parameters. We avoid GP fitting at  $z \sim 9 - 12$  due to the unavailability of low magnitude high signal-to-noise data where deviation is expected and at these redshifts, even all Schechter parameters cannot be optimised. The analysis of ten redshifts is divided into three plots. Random samples of luminosity function from the chains for Schechter function are plotted in blue lines in Figure 2 and 3. Modified functions from the Gaussian process are plotted in orange lines in the same figures. Deviations from Schechter function below magnitude  $M_{UV} = -21$  can be noticed. A similar deviation is also reported in [26]. It is important to note that most of the previous studies are based on HFF and HUDF data [20, 21, 62, 77] and others ground-based observations [32] that are limited by the magnitude larger than  $-23$ . According to those studies, Schechter function is the best description of the magnitude-luminosity relation. In our study, we combine those previous data sets with ancillary luminosity data sets of brighter galaxies ( $M_{UV} \lesssim -23$ ) from HSC data [27]. Above this magnitude, the AGN contamination to the galaxy luminosity is negligible [78–82] and therefore the previous results are consistent with our results up to certain magnitudes. The added HSC data of brighter galaxies are corrected for contribution from AGNs [27]. We find maximum excess in the bright end shape of galaxy UV LF instead of expected exponential drop of Schechter function at all redshifts where low magnitude ( $M_{UV} \lesssim -21$ ) data are available. In certain redshifts, due to high signal-to-noise ratio, the deviation is detected at high statistical significance while for other redshifts we obtain a similar deviation with lower significance. Importantly, at  $z = 3, 4$  the hyperparameters posteriors plotted in the upper left panel of Figure 4 indicate that the

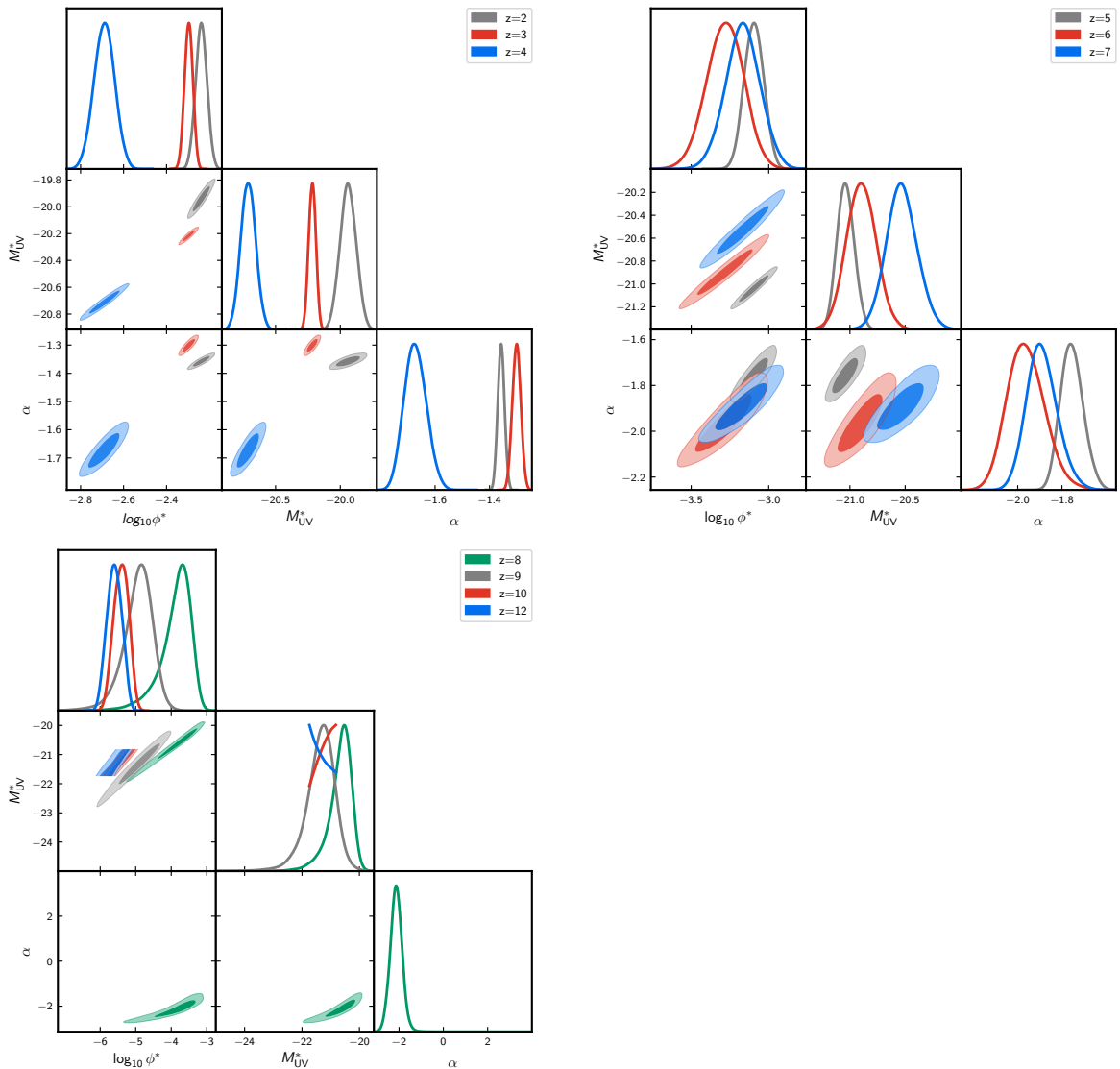


**Figure 1.** Constraints on the Schechter function parameters using galaxy luminosity data at redshifts  $z \sim 2 - 12$ .

Schechter function (used as a mean function in this analysis) is ruled out by the data at high significance. Data from  $z = 2$  and  $7$  also prefer modification over Schechter function at around  $\sim 95\%$  confidence level (C.L). In order to understand the source for this deviation, we reanalyse  $z = 4$  data with two different data cuts (with  $M_{UV} > -23$  and  $M_{UV} > -21$ ). The results are presented in the lower right panel of [Figure 4](#). When the brightest part of the observation  $-24 < M_{UV} < -23$  is not used, we notice a decrease in the significance in the GP hyperparameters ruling out Schechter function at  $3\sigma$ . When we use more conservative cuts by masking data between  $-24 < M_{UV} < -21$ , we find that further drop in significance. These tests reveal that the modifications to Schechter function are needed by the luminosity observations at the lowest magnitude (the brightest) objects.

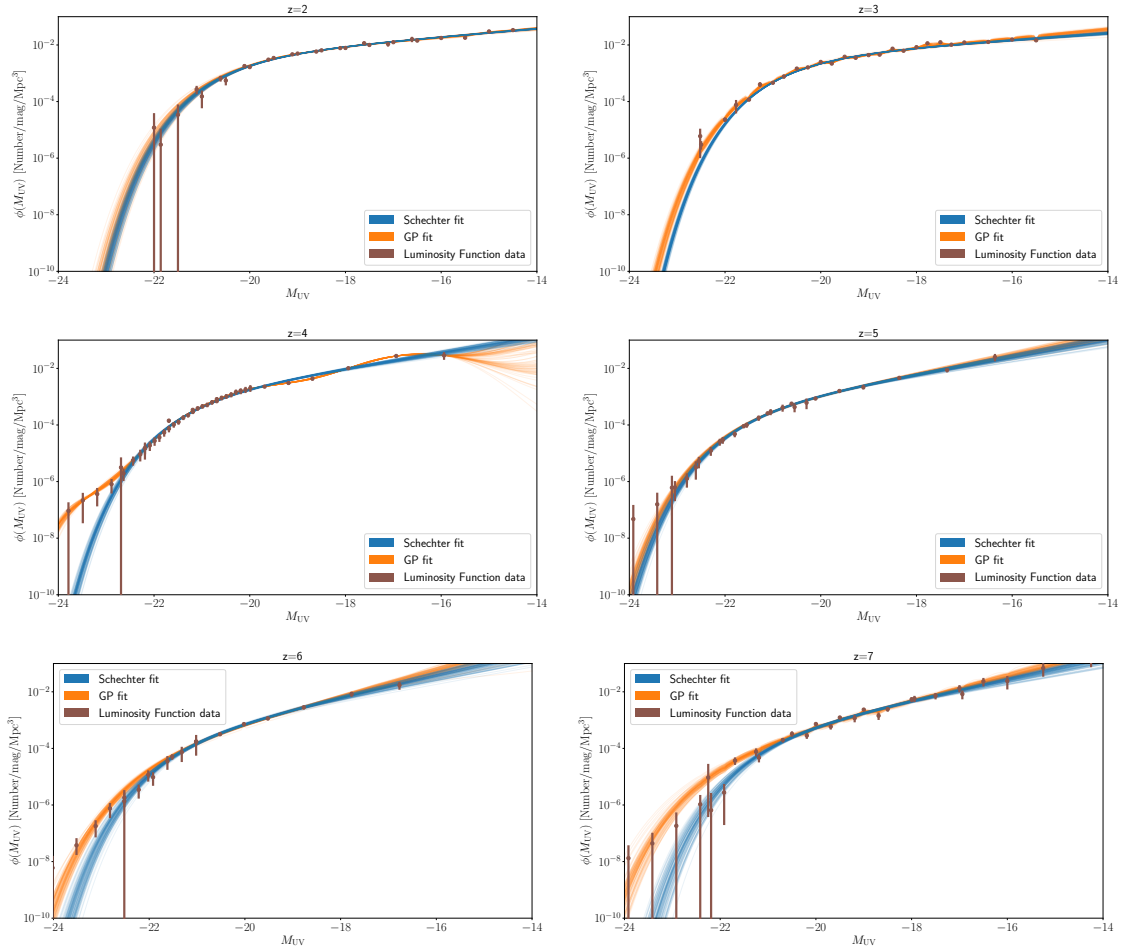


**Figure 2.** Comparison of luminosity functions from GP and Schechter function model derived from posterior samples of corresponding parameters at redshifts  $z \sim 2 - 7$ .

## 4.2 Evolution of UV Luminosity Density

We compute the UV luminosity density  $\rho_{UV}$  following Equation 2.4 integrating down to  $M_{UV} = -17$ . The samples of LFs from Schechter and GP analyses are used to estimate the posterior distribution of the derived parameter  $\rho_{UV}$ . The mean and the 68% bounds are provided in Table 1. The changes in luminosity density compared to the Schechter function model are not noticeable in the GP results. Though Schechter function is ruled out by the data at certain redshifts, the major required modifications are noticed at the brightest end of the function and the brightest end does not contribute significantly to the integral of the UV luminosity density as the function drops logarithmically with the increase in brightness. In Figure 5, we plot the redshift evolution of the luminosity density obtained from the GP (and Schechter fit) and a logarithmic double power law fit to the data (for  $z \geq 6$ ). We demonstrate only  $1\sigma$  and  $2\sigma$  spread for logarithmic double power-law fit to luminosity density obtained from the Schechter fit. We notice outliers in the data *w.r.t.* the model around redshifts 9 and 10. Recent JWST data suggests an enhanced population of star-forming Galaxies above redshifts  $z \sim 9$  [83, 84]. Compared to [56] new data may seem to hint towards a modification to the luminosity density evolution model. However, note that



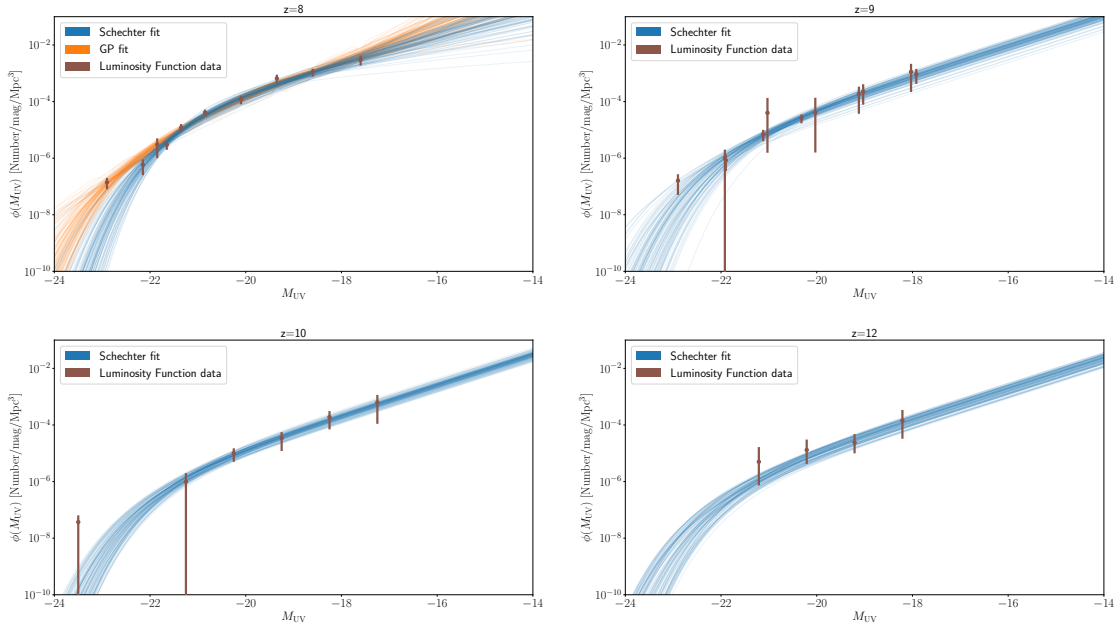


**Figure 3.** Same as Figure 2 for  $z \sim 8, 9, 10$  and  $12$ .

Model	Schechter fit				Gaussian process
	$\log_{10} \phi^*$	$M_{UV}^*$	$\alpha$	$\log_{10} \rho_{UV}$	$\log_{10} \rho_{UV}$
2	$-2.238 \pm 0.026$	$-19.940 \pm 0.061$	$-1.357 \pm 0.012$	$26.426 \pm 0.010$	$26.436 \pm 0.012$
3	$-2.297 \pm 0.019$	$-20.216 \pm 0.027$	$-1.301 \pm 0.015$	$26.4741 \pm 0.0063$	$26.489^{+0.014}_{-0.012}$
4	$-2.689 \pm 0.047$	$-20.711 \pm 0.057$	$-1.673 \pm 0.040$	$26.470 \pm 0.014$	$26.470 \pm 0.013$
5	$-3.095 \pm 0.062$	$-21.039 \pm 0.077$	$-1.755^{+0.047}_{-0.055}$	$26.264 \pm 0.019$	$26.275 \pm 0.016$
6	$-3.28 \pm 0.12$	$-20.90 \pm 0.13$	$-1.962^{+0.076}_{-0.091}$	$26.165^{+0.033}_{-0.028}$	$26.188^{+0.022}_{-0.026}$
7	$-3.17 \pm 0.11$	$-20.53 \pm 0.14$	$-1.890^{+0.062}_{-0.074}$	$26.039 \pm 0.022$	$26.071^{+0.034}_{-0.023}$
8	$-3.88^{+0.51}_{-0.23}$	$-20.68^{+0.46}_{-0.24}$	$-2.13 \pm 0.27$	$25.616^{+0.099}_{-0.066}$	$25.705 \pm 0.084$
9	$-4.94^{+0.46}_{-0.31}$	$-21.36^{+0.54}_{-0.38}$	$-2.35$	$25.12^{+0.16}_{-0.11}$	—
10	$-5.79^{+1.1}_{-0.84}$	$-21.8^{+1.6}_{-1.2}$	$-2.35$	$24.51^{+0.19}_{-0.15}$	—
12	$-6.19^{+0.67}_{-1.3}$	$< -19.1$	$-2.35$	$24.40^{+0.23}_{-0.12}$	—

**Table 1.** Constraints on luminosity density obtained from Schechter fit and the GP fit to the data at different redshifts between  $2 < z < 8$ . For  $z = 9, 10, 12$  we just provide only the Schechter fit as even the three parameters can not be constrained with two tailed distribution from the data, due to low signal-to-noise ratio.

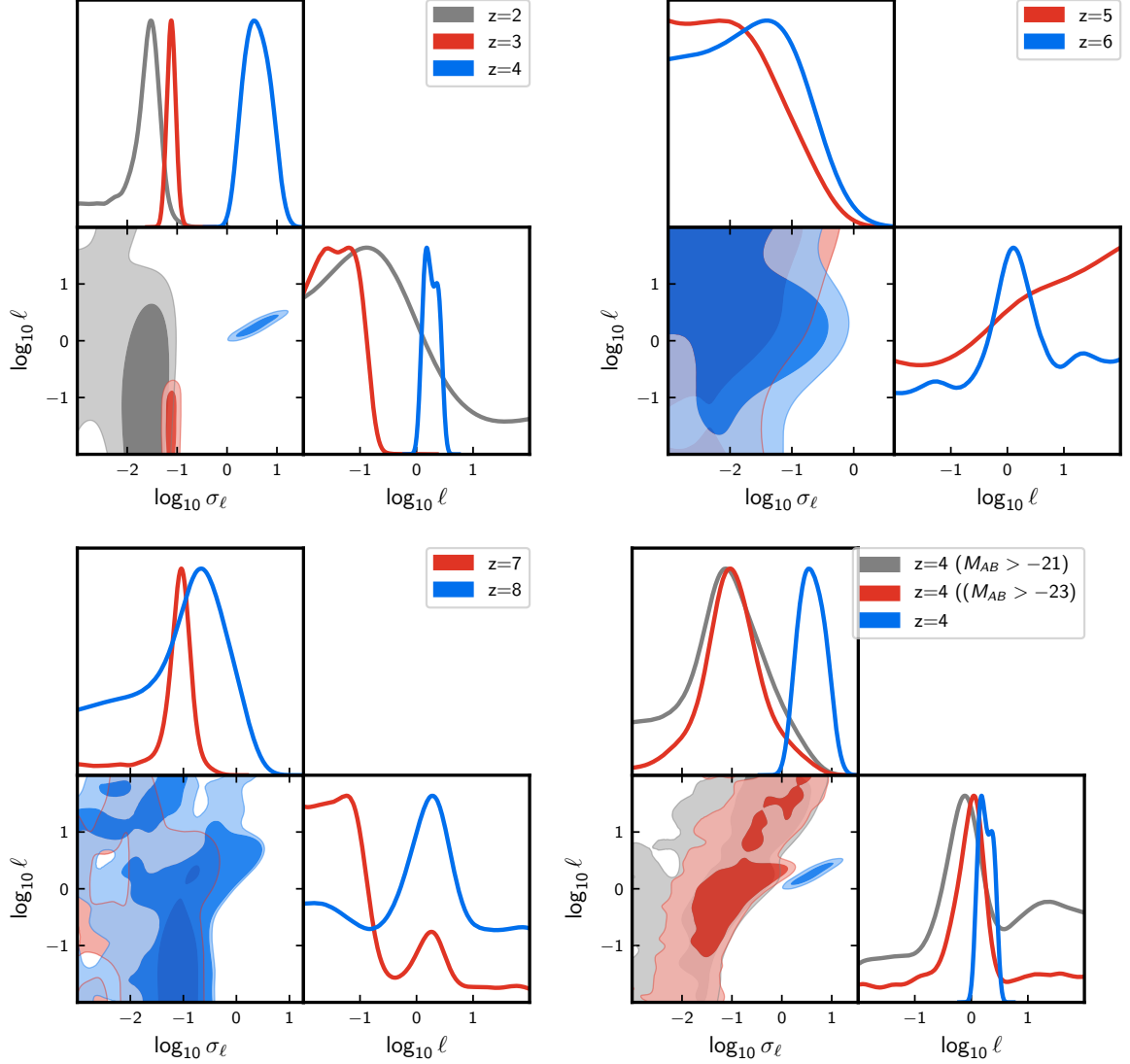


**Figure 4.** Constraints on the GP hyperparameters at different redshifts. Redshifts between  $z = 2-12$  are divided into 3 plots. At lower redshifts, mainly at  $z = 3$  and  $4$ , the data prefers significant deviation from the Schechter function. At higher redshifts, although there are some hints of deviations at  $z = 7, 8$ , they are not statistically significant. For  $z = 4$ , where we find most significant deviation, we reanalyze the data with two cuts  $M_{UV} > -23$  and  $M_{UV} > -21$  (bottom right plot). We notice that when we include the data from lower magnitudes, the Schechter function becomes increasingly inconsistent with the data.

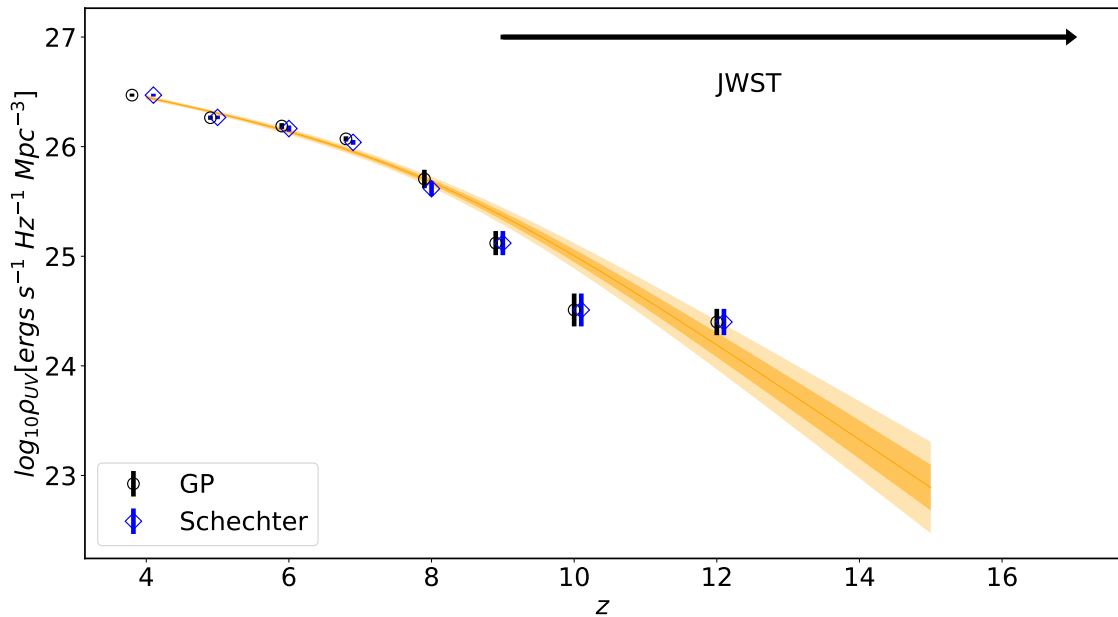


**Figure 5.** Luminosity density evolution across redshift  $z \sim 4 - 12$ . Black circles and blue diamonds are  $\rho_{UV}(z)$ s obtained from integrating the luminosity functions from GP and Schechter respectively down to the magnitude  $M_{UV} = -17$ . The orange line is best-fit logarithmic double power-law. The shaded regions are  $1\sigma$  and  $2\sigma$  confidence level to the logarithmic double power-law fit to  $\rho_{UV}$  obtained from Schechter function fit.

the data from JWST can not constrain all of the Schechter function parameters due to low signal-to-noise ratio detection, in particular, the slope remains unconstrained (see, Figure 1). This may bias the estimation of the luminosity density and therefore, with this data we avoid the exploration for the possible deviation from the double power law model. We expect to revisit this issue in the future when new data from JWST are made available.

### 4.3 Constraints on Reionization

We obtain the constraint on redshift evolution of IGM neutral hydrogen fraction from joint fitting of Planck data,  $Q_{\text{HII}}$  data, and UV luminosity density data derived in subsection 4.2. We treat the four parameters in logarithmic double power-law form of  $\rho_{UV}$  and  $\log_{10}\langle f_{\text{esc}}\xi_{\text{ion}}\rangle$  as free parameters. For  $C_{\text{HII}}$  we use a fixed value of 3.

In Figure 6 we compare the  $Q_{\text{HII}}$  evolution across redshift  $z \sim 4-15$  solving Equation 2.1 using  $\rho_{UV}$  data sets obtained from both parametric and non-parametric methods. The blue dashed line and magenta solid line are the best fit  $Q_{\text{HII}}$  obtained with  $\rho_{UV}$  from GP and Schechter fits respectively. The grey and cyan lines indicate random samples of  $Q_{\text{HII}}$  obtained from these fits respectively. We also overplot the  $Q_{\text{HII}}$  data set used in our analysis. Both the  $\rho_{UV}$  data sets provide similar constraints on reionization history. This is not surprising as we discussed that the obtained luminosity density follows similar redshift evolution owing to the similar nature of luminosity functions at the faint source end. This result suggests that the reionization process is mainly driven by fainter galaxies. The excess dropout galaxies at the brighter-end of magnitude have limited contribution to the reionization process due to

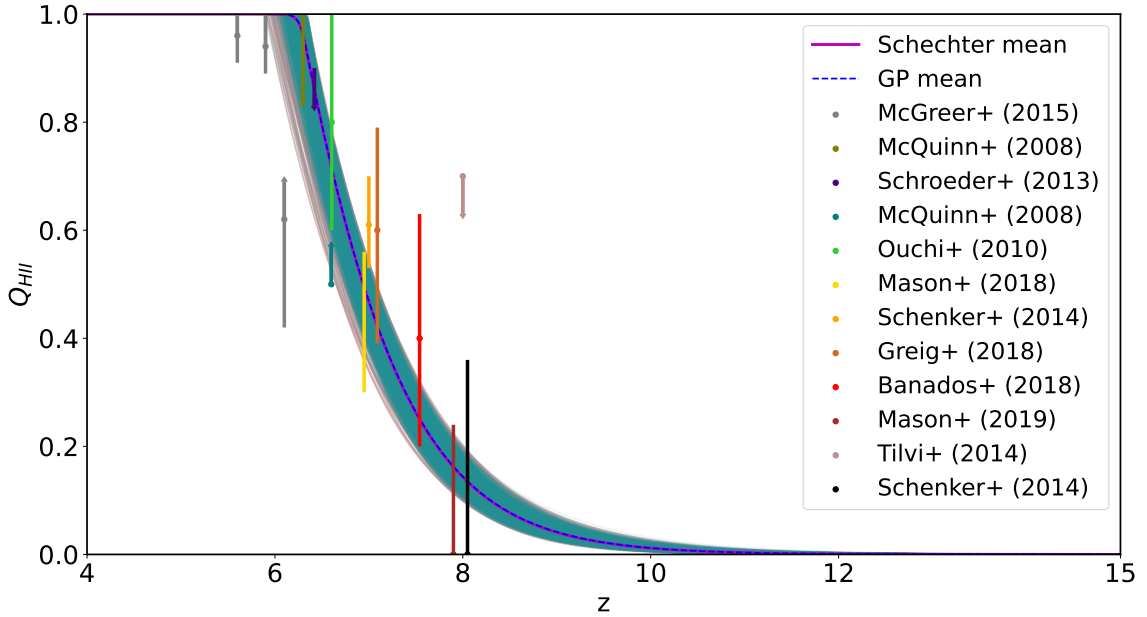


**Figure 6.** Redshift evolution of  $Q_{\text{HII}}$  across  $z \sim 4 - 15$ . The dashed blue and solid magenta lines are best-fit  $Q_{\text{HII}}$  estimated using  $\rho_{\text{UVS}}$  from GP and Schechter functions respectively. The gray (cyan) curves are random samples of  $Q_{\text{HII}}$  for these two respective cases. The  $Q_{\text{HII}}$  data sets used for joint fitting are also shown.

lower number density or possibly low escape fraction. Earlier publications in [11, 48, 85–87] reached to a similar conclusions using model-based reionization study. As shown in Figure 6 we find much tighter bound of  $Q_{\text{HII}}$  as compared to previous works in [51, 54, 56, 85, 86]. We quote the midpoint (50%) redshift of reionization  $z_{\text{re}}$  in Table 2 which is less than the Planck reported value [4]. Our constraints on the duration of reionization (redshift difference between 10% to 90% reionization) are  $\Delta z \sim 1.627_{-0.071}^{+0.059}$  and  $1.627_{-0.070}^{+0.060}$  with 68% confidence interval using Schechter function and GP based  $\rho_{\text{UV}}$  data sets respectively. This is consistent with a upper bound of  $\Delta z < 2.8$  as reported in [88] from the Kinetic Sunyaev–Zel’dovich effect. This implies our values suggest a sharper reionization history. Finally our constrain on reionization optical depth is  $\tau_{\text{re}} = 0.0492_{-0.0006}^{+0.0008}$  and  $0.0494_{-0.0006}^{+0.0007}$  from Schechter and GP analyses. These values are also listed in Table 2. However, we would like to highlight here that the uncertainties in the reionization histories quoted in this subsection are underestimated as we have fixed both the clumping factor and the escape fraction in our analyses. Therefore, these summary statistics on optical depth and the duration of reionization should be used with caution in any subsequent analysis. The exercise in this subsection has been performed to indicate that the constraints on the cosmology remain unaltered even though Schechter function is ruled out by the observational data. The flattening/increase in the luminosity density data at high redshifts as indicated by the JWST data in this analysis does not show an impact in the optical depth constraints as – (1) we have not used the very high redshift observations ( $z \sim 14, 16$ ) from JWST, and (2) the double power-law form used for the luminosity density does not capture its increasing trend at high redshifts.

	using $\log_{10}[\rho_{\text{UV}}]$ from Schechter	using $\log_{10}[\rho_{\text{UV}}]$ from GP
$\tau_{\text{re}}$	$0.0492^{+0.0008}_{-0.0006}$	$0.0494^{+0.0007}_{-0.0006}$
$z_{\text{re}}$	$6.778^{+0.054}_{-0.029}$	$6.777^{+0.055}_{-0.028}$
$\Delta z$	$1.627^{+0.059}_{-0.071}$	$1.627^{+0.060}_{-0.070}$

**Table 2.** Summary of constraints on reionization history using  $\rho_{\text{UV}}$  data sets obtained from both parametric and non-parametric methods.

## 5 Summary

In this paper, we investigate the UV luminosity functions between redshifts  $z \sim 2 - 12$  over a wide range of magnitude  $-25 \lesssim M_{\text{UV}} \lesssim -14$  based on HST, HSC and JWST data sets. We test whether the conventional Schechter function is a valid theoretical model that can address the data for such a wide range of magnitudes and redshifts and what are the implications of any modified function to the reionization history.

We fit both commonly used Schechter function model at all redshifts  $z \sim 2 - 12$  and perform a free-form reconstruction at redshifts  $z \sim 2 - 8$  using Gaussian process to the same data sets. We find although Schechter function is a very good description of the dropout galaxies for the fainter end of magnitude ( $M_{\text{UV}} \gtrsim -21$ ), its exponential tail is inconsistent with brighter dropout galaxies at almost all redshifts where low magnitude data are available. The Gaussian process regression allows a free-form reconstruction of UV LFs and therefore can well describe the excess LF at the bright-end which is not possible to address with Schechter function. We obtain the UV luminosity densities integrating over both LF forms down to the magnitude  $M_{\text{UV}} = -17$ . Since at the fainter end of the magnitude, Schechter function is consistent with the data and the fainter end contributes dominantly to the luminosity density integral due to the maximum availability of Galaxies, we find similar luminosity densities in both the methods. Therefore, reionization history is found to be similar in both cases. This implies that brighter dropout galaxies have insignificant contributions in reionization process (supported by earlier publications as well). However, integrating to more fainter sources  $M_{\text{UV}} > -15$  can indicate certain differences which we do not explore by considering  $M_{\text{UV}} = -17$  as the conservative choice.

The data at redshifts 9, 10 and 12 do not have a high signal-to-noise ratio and therefore can not constrain all the Schechter function parameters. Therefore testing a modification to Schechter function is beyond the scope of this paper with the available data. More observational data from JWST NIRSspec will be required for further studies at higher redshifts. Furthermore, we have not incorporated redshift dependencies of clumping factor and escape fraction into our simplistic reionization model and also neglect the contributions from quasars as reionization sources which could potentially enhance the accuracy of our findings. It would be intriguing to incorporate all these modifications into our model and reassess the current analysis when new data from JWST and other sources with significant improvement in the signal-to-noise ratio are made available. We defer these extensions for future investigations.

## 6 Acknowledgement

All the computations in this paper are done using the HPC Nandadevi and Kamet (<https://hpc.imsc.res.in>) at the Institute of Mathematical Sciences, Chennai, India. The authors would like to thank Yuichi Harikane for providing the UV luminosity data sets used in this work. DKH would like to thank Daniela Paoletti for certain important discussions. DKH would like to acknowledge the support from the Indo-French Centre for the Promotion of Advanced Research – CEFIPRA grant no. 6704-4 and the support through the India-Italy “RELIC - Reconstructing Early and Late events In Cosmology” mobility program.

## References

- [1] X. Fan, M.A. Strauss, R.H. Becker, R.L. White, J.E. Gunn, G.R. Knapp et al., *Constraining the Evolution of the Ionizing Background and the Epoch of Reionization with  $z \sim 6$  Quasars. II. A Sample of 19 Quasars*, *AJ* **132** (2006) 117 [[astro-ph/0512082](#)].
- [2] I.D. McGreer, A. Mesinger and V. D’Odorico, *Model-independent evidence in favour of an end to reionization by  $z \approx 6$* , *MNRAS* **447** (2015) 499 [[1411.5375](#)].
- [3] D.K. Hazra and G.F. Smoot, *Witnessing the reionization history using cosmic microwave background observation from planck*, *Journal of Cosmology and Astroparticle Physics* **2017** (2017) 028.
- [4] Planck Collaboration, N. Aghanim, Y. Akrami, M. Ashdown, J. Aumont, C. Baccigalupi et al., *Planck 2018 results. VI. Cosmological parameters*, *A&A* **641** (2020) A6 [[1807.06209](#)].
- [5] D. Paoletti, D.K. Hazra, F. Finelli and G.F. Smoot, *The asymmetry of dawn: evidence for asymmetric reionization histories from a joint analysis of cosmic microwave background and astrophysical data*, [2405.09506](#).
- [6] G. Worseck, J.X. Prochaska, J.F. Hennawi and M. McQuinn, *Early and Extended Helium Reionization over More Than 600 Million Years of Cosmic Time*, *ApJ* **825** (2016) 144 [[1405.7405](#)].
- [7] A. Fontana, E. Vanzella, L. Pentericci, M. Castellano, M. Giavalisco, A. Grazian et al., *The Lack of Intense Ly $\alpha$  in Ultradeep Spectra of  $z = 7$  Candidates in GOODS-S: Imprint of Reionization?*, *ApJ* **725** (2010) L205 [[1010.2754](#)].
- [8] C.J. Willott, P. Delorme, C. Reyl e, L. Albert, J. Bergeron, D. Crampton et al., *The Canada-France High- $z$  Quasar Survey: Nine New Quasars and the Luminosity Function at Redshift 6*, *AJ* **139** (2010) 906 [[0912.0281](#)].
- [9] M. Onoue, N. Kashikawa, C.J. Willott, P. Hibon, M. Im, H. Furusawa et al., *Minor Contribution of Quasars to Ionizing Photon Budget at  $z \sim 6$ : Update on Quasar Luminosity Function at the Faint End with Subaru/Suprime-Cam*, *ApJ* **847** (2017) L15 [[1709.04413](#)].
- [10] S. Hassan, R. Dav e, S. Mitra, K. Finlator, B. Ciardi and M.G. Santos, *Constraining the contribution of active galactic nuclei to reionization*, *Monthly Notices of the Royal Astronomical Society* **473** (2017) 227 [<https://academic.oup.com/mnras/article-pdf/473/1/227/21308514/stx2194.pdf>].
- [11] P. Dayal, M. Volonteri, T.R. Choudhury, R. Schneider, M. Trebitsch, N.Y. Gnedin et al., *Reionization with galaxies and active galactic nuclei*, *MNRAS* **495** (2020) 3065 [[2001.06021](#)].
- [12] C. Liu, S.J. Mutch, P.W. Angel, A.R. Duffy, P.M. Geil, G.B. Poole et al., *Dark-ages reionization and galaxy formation simulation – IV. UV luminosity functions of high-redshift galaxies*, *Monthly Notices of the Royal Astronomical Society* **462** (2016) 235 [<https://academic.oup.com/mnras/article-pdf/462/1/235/18468542/stw1015.pdf>].

- [13] T.R. Choudhury and A. Ferrara, *Experimental constraints on self-consistent reionization models*, *Monthly Notices of the Royal Astronomical Society* **361** (2005) 577 [<https://academic.oup.com/mnras/article-pdf/361/2/577/18660784/361-2-577.pdf>].
- [14] B.E. Robertson, *Estimating Luminosity Function Constraints from High-Redshift Galaxy Surveys*, *ApJ* **713** (2010) 1266 [1001.1008].
- [15] J.M. Lotz, A. Koekemoer, D. Coe, N. Grogin, P. Capak, J. Mack et al., *The Frontier Fields: Survey Design and Initial Results*, *ApJ* **837** (2017) 97 [1605.06567].
- [16] M.A. Schenker, B.E. Robertson, R.S. Ellis, Y. Ono, R.J. McLure, J.S. Dunlop et al., *The uv luminosity function of star-forming galaxies via dropout selection at redshifts  $z \sim 7$  and 8 from the 2012 ultra deep field campaign*, *The Astrophysical Journal* **768** (2013) 196.
- [17] R.S. Ellis, R.J. McLure, J.S. Dunlop, B.E. Robertson, Y. Ono, M.A. Schenker et al., *The Abundance of Star-forming Galaxies in the Redshift Range 8.5-12: New Results from the 2012 Hubble Ultra Deep Field Campaign*, *ApJ* **763** (2013) L7 [1211.6804].
- [18] R.J. McLure, J.S. Dunlop, R.A.A. Bowler, E. Curtis-Lake, M. Schenker, R.S. Ellis et al., *A new multifield determination of the galaxy luminosity function at  $z = 7-9$  incorporating the 2012 Hubble Ultra-Deep Field imaging*, *Monthly Notices of the Royal Astronomical Society* **432** (2013) 2696 [<https://academic.oup.com/mnras/article-pdf/432/4/2696/9501883/stt627.pdf>].
- [19] M. Ishigaki, R. Kawamata, M. Ouchi, M. Oguri, K. Shimasaku and Y. Ono, *Hubble Frontier Fields First Complete Cluster Data: Faint Galaxies at  $z \sim 5 - 10$  for UV Luminosity Functions and Cosmic Reionization*, *Astrophys. J.* **799** (2015) 12 [1408.6903].
- [20] M. Ishigaki, R. Kawamata, M. Ouchi, M. Oguri, K. Shimasaku and Y. Ono, *Full-data Results of Hubble Frontier Fields: UV Luminosity Functions at  $z \sim 6 - 10$  and a Consistent Picture of Cosmic Reionization*, *ApJ* **854** (2018) 73 [1702.04867].
- [21] R.J. Bouwens et al., *UV Luminosity Functions at redshifts  $z \sim 4$  to  $z \sim 10$ : 10000 Galaxies from HST Legacy Fields*, *Astrophys. J.* **803** (2015) 34 [1403.4295].
- [22] P. Schechter, *An analytic expression for the luminosity function for galaxies.*, *ApJ* **203** (1976) 297.
- [23] J. Loveday, P. Norberg, I.K. Baldry, S.P. Driver, A.M. Hopkins, J.A. Peacock et al., *Galaxy and Mass Assembly (GAMA): ugriz galaxy luminosity functions*, *Monthly Notices of the Royal Astronomical Society* **420** (2012) 1239 [<https://academic.oup.com/mnras/article-pdf/420/2/1239/3065107/mnras0420-1239.pdf>].
- [24] R.G. Bower, A.J. Benson, R. Malbon, J.C. Helly, C.S. Frenk, C.M. Baugh et al., *Breaking the hierarchy of galaxy formation*, *Monthly Notices of the Royal Astronomical Society* **370** (2006) 645 [<https://academic.oup.com/mnras/article-pdf/370/2/645/2898993/mnras0370-0645.pdf>].
- [25] A.J. Benson, R.G. Bower, C.S. Frenk, C.G. Lacey, C.M. Baugh and S. Cole, *What Shapes the Luminosity Function of Galaxies?*, *ApJ* **599** (2003) 38 [astro-ph/0302450].
- [26] Y. Ono, M. Ouchi, Y. Harikane, J. Toshikawa, M. Rauch, S. Yuma et al., *Great Optically Luminous Dropout Research Using Subaru HSC (GOLDRUSH). I. UV luminosity functions at  $z \sim 4-7$  derived with the half-million dropouts on the 100 deg<sup>2</sup> sky*, *PASJ* **70** (2018) S10 [1704.06004].
- [27] Y. Harikane, A.K. Inoue, K. Mawatari, T. Hashimoto, S. Yamanaka, Y. Fudamoto et al., *A search for h-dropout lyman break galaxies at  $z \sim 12 - 16$* , *The Astrophysical Journal* **929** (2022) 1.
- [28] R.A.A. Bowler, J.S. Dunlop, R.J. McLure, H.J. McCracken, B. Milvang-Jensen, H. Furusawa et al., *Discovery of bright  $z \simeq 7$  galaxies in the UltraVISTA survey*, *Monthly Notices of the*

- Royal Astronomical Society* **426** (2012) 2772  
[\[https://academic.oup.com/mnras/article-pdf/426/4/2772/3299565/426-4-2772.pdf\]](https://academic.oup.com/mnras/article-pdf/426/4/2772/3299565/426-4-2772.pdf).
- [29] J.S.B. Wyithe, H. Yan, R.A. Windhorst and S. Mao, *A distortion of very-high-redshift galaxy number counts by gravitational lensing*, *Nature* **469** (2011) 181 [1101.2291].
- [30] J. Rigby, M. Perrin, M. McElwain, R. Kimble, S. Friedman, M. Lallo et al., *The Science Performance of JWST as Characterized in Commissioning*, *PASP* **135** (2023) 048001 [2207.05632].
- [31] M. Stefanon, I. Labbé, R.J. Bouwens, P. Oesch, M.L.N. Ashby, K.I. Caputi et al., *The Brightest  $z \gtrsim 8$  Galaxies over the COSMOS UltraVISTA Field*, *ApJ* **883** (2019) 99 [1902.10713].
- [32] R.A.A. Bowler, M.J. Jarvis, J.S. Dunlop, R.J. McLure, D.J. McLeod, N.J. Adams et al., *A lack of evolution in the very bright end of the galaxy luminosity function from  $z \simeq 8$  to 10*, *MNRAS* **493** (2020) 2059 [1911.12832].
- [33] M.L. Stevans, S.L. Finkelstein, I. Wold, L. Kawinwanichakij, C. Papovich, S. Sherman et al., *Bridging Star-forming Galaxy and AGN Ultraviolet Luminosity Functions at  $z = 4$  with the SHELA Wide-field Survey*, *ApJ* **863** (2018) 63 [1806.05187].
- [34] N.J. Adams, R.A.A. Bowler, M.J. Jarvis, B. Häußler, R.J. McLure, A. Bunker et al., *The rest-frame UV luminosity function at  $z \simeq 4$ : a significant contribution of AGNs to the bright end of the galaxy population*, *MNRAS* **494** (2020) 1771 [1912.01626].
- [35] R. Barkana and A. Loeb, *In the beginning: the first sources of light and the reionization of the universe*, *Phys. Rep.* **349** (2001) 125 [astro-ph/0010468].
- [36] M. Kuhlen and C.-A. Faucher-Giguère, *Concordance models of reionization: implications for faint galaxies and escape fraction evolution*, *Monthly Notices of the Royal Astronomical Society* **423** (2012) 862 [https://academic.oup.com/mnras/article-pdf/423/1/862/18612580/mnras0423-0862.pdf].
- [37] B.E. Robertson, S.R. Furlanetto, E. Schneider, S. Charlot, R.S. Ellis, D.P. Stark et al., *New Constraints on Cosmic Reionization from the 2012 Hubble Ultra Deep Field Campaign*, *ApJ* **768** (2013) 71 [1301.1228].
- [38] I.T. Iliev, G. Mellema, U.L. Pen, H. Merz, P.R. Shapiro and M.A. Alvarez, *Simulating cosmic reionization at large scales - I. The geometry of reionization*, *MNRAS* **369** (2006) 1625 [astro-ph/0512187].
- [39] A.H. Pawlik, J. Schaye and E. van Scherpenzeel, *Keeping the Universe ionized: photoheating and the clumping factor of the high-redshift intergalactic medium*, *MNRAS* **394** (2009) 1812 [0807.3963].
- [40] K. Finlator, S.P. Oh, F. Özel and R. Davé, *Gas clumping in self-consistent reionization models*, *Monthly Notices of the Royal Astronomical Society* **427** (2012) 2464 [https://academic.oup.com/mnras/article-pdf/427/3/2464/3857876/427-3-2464.pdf].
- [41] J. Schroeder, A. Mesinger and Z. Haiman, *Evidence of Gunn-Peterson damping wings in high- $z$  quasar spectra: strengthening the case for incomplete reionization at  $z \sim 6-7$* , *MNRAS* **428** (2013) 3058 [1204.2838].
- [42] J.M. Shull, A. Harness, M. Trenti and B.D. Smith, *Critical star formation rates for reionization: Full reionization occurs at redshift  $z = 7$* , *The Astrophysical Journal* **747** (2012) 100.
- [43] B.E. Robertson, *Galaxy formation and reionization: Key unknowns and expected breakthroughs by the James Webb Space Telescope*, *Annual Review of Astronomy and Astrophysics* **60** (2022) 121 [https://doi.org/10.1146/annurev-astro-120221-044656].
- [44] A.K. Inoue, I. Shimizu, I. Iwata and M. Tanaka, *An updated analytic model for attenuation by the intergalactic medium*, *MNRAS* **442** (2014) 1805 [1402.0677].



- [45] E.R. Fernandez and J.M. Shull, *The effect of galactic properties on the escape fraction of ionizing photons*, *The Astrophysical Journal* **731** (2011) 20.
- [46] C.A. Mason, T. Treu, M. Dijkstra, A. Mesinger, M. Trenti, L. Pentericci et al., *The Universe Is Reionizing at  $z \sim 7$ : Bayesian Inference of the IGM Neutral Fraction Using Ly $\alpha$  Emission from Galaxies*, *Astrophys. J.* **856** (2018) 2 [1709.05356].
- [47] X. Ma, D. Kasen, P.F. Hopkins, C.-A. Faucher-Giguère, E. Quataert, D. KereÅi et al., *The difficulty of getting high escape fractions of ionizing photons from high-redshift galaxies: a view from the FIRE cosmological simulations*, *Monthly Notices of the Royal Astronomical Society* **453** (2015) 960 [https://academic.oup.com/mnras/article-pdf/453/1/960/4935561/stv1679.pdf].
- [48] H. Atek, I. Labbé, L.J. Furtak, I. Chemerynska, S. Fujimoto, D.J. Setton et al., *Most of the photons that reionized the Universe came from dwarf galaxies*, *Nature* **626** (2024) 975 [2308.08540].
- [49] C. Simmonds, S. Tacchella, K. Hainline, B.D. Johnson, W. McClymont, B. Robertson et al., *Low-mass bursty galaxies in JADES efficiently produce ionizing photons and could represent the main drivers of reionization*, *MNRAS* **527** (2024) 6139 [2310.01112].
- [50] J.B. Muñoz, J. Mirocha, J. Chisholm, S.R. Furlanetto and C. Mason, *Reionization after JWST: a photon budget crisis?*, *arXiv e-prints* (2024) arXiv:2404.07250 [2404.07250].
- [51] S. Mitra and A. Chatterjee, *Non-parametric reconstruction of photon escape fraction from reionization*, *MNRAS* **523** (2023) L35 [2303.02704].
- [52] C.-A. Faucher-Giguère, D. KereÅi and C.-P. Ma, *The baryonic assembly of dark matter haloes*, *Monthly Notices of the Royal Astronomical Society* **417** (2011) 2982 [https://academic.oup.com/mnras/article-pdf/417/4/2982/3842290/mnras0417-2982.pdf].
- [53] Y.-W. Yu, K. Cheng, M. Chu and S. Yeung, *Cosmic histories of star formation and reionization: an analysis with a power-law approximation*, *Journal of Cosmology and Astroparticle Physics* **2012** (2012) 023.
- [54] D.K. Hazra, D. Paoletti, F. Finelli and G.F. Smoot, *Joining bits and pieces of reionization history*, *Phys. Rev. Lett.* **125** (2020) 071301.
- [55] D. Paoletti, D.K. Hazra, F. Finelli and G.F. Smoot, *Extended reionization in models beyond  $\Lambda$ CDM with Planck 2018 data*, *JCAP* **09** (2020) 005 [2005.12222].
- [56] A. Krishak and D.K. Hazra, *Gaussian process reconstruction of reionization history*, *The Astrophysical Journal* **922** (2021) 95.
- [57] D. Paoletti, D.K. Hazra, F. Finelli and G.F. Smoot, *Dark twilight joined with the light of dawn to unveil the reionization history*, *Phys. Rev. D* **104** (2021) 123549 [2107.10693].
- [58] M. Seikel, C. Clarkson and M. Smith, *Reconstruction of dark energy and expansion dynamics using gaussian processes*, *Journal of Cosmology and Astroparticle Physics* **2012** (2012) 036.
- [59] A. Shafieloo, A.G. Kim and E.V. Linder, *Model independent tests of cosmic growth versus expansion*, *Phys. Rev. D* **87** (2013) 023520.
- [60] R. Calderon, A. Shafieloo, D. Kumar Hazra and W. Sohn, *On the consistency of  $\Lambda$ CDM with CMB measurements in light of the latest Planck, ACT and SPT data*, *J. Cosmology Astropart. Phys.* **2023** (2023) 059 [2302.14300].
- [61] C.E. Rasmussen and C.K.I. Williams, *Gaussian processes for machine learning.*, Adaptive computation and machine learning, MIT Press (2006).
- [62] R.J. Bouwens, P.A. Oesch, M. Stefanon, G. Illingworth, I. Labbé, N. Reddy et al., *New Determinations of the UV Luminosity Functions from  $z$  9 to 2 Show a Remarkable Consistency with Halo Growth and a Constant Star Formation Efficiency*, *AJ* **162** (2021) 47 [2102.07775].

- [63] Y. Harikane, Y. Ono, M. Ouchi, C. Liu, M. Sawicki, T. Shibuya et al., *GOLDRUSH. IV. Luminosity Functions and Clustering Revealed with 4,000,000 Galaxies at  $z \sim 2-7$ : Galaxy-AGN Transition, Star Formation Efficiency, and Implication for Evolution at  $z \lesssim 10$* , *ApJS* **259** (2022) 20 [2108.01090].
- [64] P.A. Oesch, R.J. Bouwens, G.D. Illingworth, I. Labbé and M. Stefanon, *The dearth of  $z \sim 10$  galaxies in all hst legacy fields—the rapid evolution of the galaxy population in the first 500 myr*, *The Astrophysical Journal* **855** (2018) 105.
- [65] D.J. McLeod, R.J. McLure and J.S. Dunlop, *The  $z = 9-10$  galaxy population in the Hubble Frontier Fields and CLASH surveys: the  $z = 9$  luminosity function and further evidence for a smooth decline in ultraviolet luminosity density at  $z \geq 8$* , *MNRAS* **459** (2016) 3812 [1602.05199].
- [66] Y. Harikane, M. Ouchi, M. Oguri, Y. Ono, K. Nakajima, Y. Isobe et al., *A Comprehensive Study of Galaxies at  $z \sim 9-16$  Found in the Early JWST Data: Ultraviolet Luminosity Functions and Cosmic Star Formation History at the Pre-reionization Epoch*, *ApJS* **265** (2023) 5 [2208.01612].
- [67] Y. Ono et al., *Spectroscopic Confirmation of Three  $z$ -Dropout Galaxies at  $z = 6.844 - 7.213$ : Demographics of Lyman-Alpha Emission in  $z \sim 7$  Galaxies*, *Astrophys. J.* **744** (2012) 83 [1107.3159].
- [68] V. Tilvi, C. Papovich, S.L. Finkelstein, J. Long, M. Song, M. Dickinson et al., *Rapid Decline of Ly $\alpha$  Emission Toward the Reionization Era*, *Astrophys. J.* **794** (2014) 5 [1405.4869].
- [69] M.A. Schenker, R.S. Ellis, N.P. Konidakis and D.P. Stark, *Line Emitting Galaxies Beyond a Redshift of 7: An Improved Method for Estimating the Evolving Neutrality of the Intergalactic Medium*, *Astrophys. J.* **795** (2014) 20 [1404.4632].
- [70] B. Greig, A. Mesinger, Z. Haiman and R.A. Simcoe, *Are we witnessing the epoch of reionization at  $z=7.1$  from the spectrum of J1120+0641?*, *Mon. Not. Roy. Astron. Soc.* **466** (2017) 4239 [1606.00441].
- [71] F.B. Davies et al., *Quantitative Constraints on the Reionization History from the IGM Damping Wing Signature in Two Quasars at  $z \lesssim 7$* , *Astrophys. J.* **864** (2018) 142 [1802.06066].
- [72] T. Totani, N. Kawai, G. Kosugi, K. Aoki, T. Yamada, M. Iye et al., *Implications for the cosmic reionization from the optical afterglow spectrum of the gamma-ray burst 050904 at  $z = 6.3$* , *Publ. Astron. Soc. Jap.* **58** (2006) 485 [astro-ph/0512154].
- [73] M. McQuinn, A. Lidz, M. Zaldarriaga, L. Hernquist and S. Dutta, *Probing the neutral fraction of the IGM with GRBs during the epoch of reionization*, *MNRAS* **388** (2008) 1101 [0710.1018].
- [74] J.S. Bolton, M.G. Haehnelt, S.J. Warren, P.C. Hewett, D.J. Mortlock, B.P. Venemans et al., *How neutral is the intergalactic medium surrounding the redshift  $z = 7.085$  quasar ULAS J1120+0641?*, *MNRAS* **416** (2011) L70 [1106.6089].
- [75] D.J. Mortlock, S.J. Warren, B.P. Venemans, M. Patel, P.C. Hewett, R.G. McMahon et al., *A luminous quasar at a redshift of  $z = 7.085$* , *Nature* **474** (2011) 616 [1106.6088].
- [76] A. Lewis and S. Bridle, *Cosmological parameters from CMB and other data: A Monte Carlo approach*, *Phys. Rev.* **D66** (2002) 103511 [astro-ph/0205436].
- [77] S.L. Finkelstein, R.E. Ryan, C. Papovich, M. Dickinson, M. Song, R.S. Somerville et al., *The evolution of the galaxy rest-frame ultraviolet luminosity function over the first two billion years*, *The Astrophysical Journal* **810** (2015) 71.
- [78] E. Glikman, S.G. Djorgovski, D. Stern, A. Dey, B.T. Jannuzi and K.-S. Lee, *The faint end of the quasar luminosity function at  $z \sim 4$ : Implications for ionization of the intergalactic medium and cosmic downsizing\**, *The Astrophysical Journal Letters* **728** (2011) L26.

- [79] E. Giallongo, A. Grazian, F. Fiore, A. Fontana, L. Pentericci, E. Vanzella et al., *Faint AGNs at  $z \gtrsim 4$  in the CANDELS GOODS-S field: looking for contributors to the reionization of the Universe*, *A&A* **578** (2015) A83 [1502.02562].
- [80] M. Niida, T. Nagao, H. Ikeda, K. Matsuoka, M.A.R. Kobayashi, Y. Toba et al., *Revisiting the completeness and luminosity function in high-redshift low-luminosity quasar surveys*, *The Astrophysical Journal* **832** (2016) 208.
- [81] M. Akiyama, W. He, H. Ikeda, M. Niida, T. Nagao, J. Bosch et al., *The quasar luminosity function at redshift 4 with the Hyper Suprime-Cam Wide Survey*, *Publications of the Astronomical Society of Japan* **70** (2017) [https://academic.oup.com/pasj/article-pdf/70/SP1/S34/23692427/psx091.pdf].
- [82] S. Parsa, J.S. Dunlop and R.J. McLure, *No evidence for a significant AGN contribution to cosmic hydrogen reionization*, *Monthly Notices of the Royal Astronomical Society* **474** (2017) 2904 [https://academic.oup.com/mnras/article-pdf/474/3/2904/22843311/stx2887.pdf].
- [83] S.L. Finkelstein, M.B. Bagley, H.C. Ferguson, S.M. Wilkins, J.S. Kartaltepe, C. Papovich et al., *CEERS Key Paper. I. An Early Look into the First 500 Myr of Galaxy Formation with JWST*, *ApJ* **946** (2023) L13 [2211.05792].
- [84] D.J. Eisenstein, C. Willott, S. Alberts, S. Arribas, N. Bonaventura, A.J. Bunker et al., *Overview of the JWST Advanced Deep Extragalactic Survey (JADES)*, *arXiv e-prints* (2023) arXiv:2306.02465 [2306.02465].
- [85] S. Mitra, T.R. Choudhury and A. Ferrara, *Cosmic reionization after Planck.*, *MNRAS* **454** (2015) L76 [1505.05507].
- [86] S. Mitra, T.R. Choudhury and B. Ratra, *First study of reionization in the Planck 2015 normalized closed  $\Lambda$ CDM inflation model*, *MNRAS* **479** (2018) 4566 [1712.00018].
- [87] S.L. Finkelstein, A. D'Aloisio, J.-P. Paardekooper, J. Ryan, Russell, P. Behroozi, K. Finlator et al., *Conditions for Reionizing the Universe with a Low Galaxy Ionizing Photon Escape Fraction*, *ApJ* **879** (2019) 36 [1902.02792].
- [88] Planck Collaboration, R. Adam, N. Aghanim, M. Ashdown, J. Aumont, C. Baccigalupi et al., *Planck intermediate results. XLVII. Planck constraints on reionization history*, *A&A* **596** (2016) A108 [1605.03507].